Phase-Shift-Based Time-Delay Estimators for Proximity Acoustic Sensors

Xi Li, *Student Member, IEEE*, Erik G. Larsson, Mark Sheplak, and Jian Li, *Senior Member, IEEE*

***Abstract*—Time-delay estimation is important in a wide range of applications in oceanic engineering. In this paper, we present a novel time-delay estimation algorithm based on maximum likelihood theory for the case that the measurements are corrupted by colored or nonuniform zero-mean Gaussian noise. It turns out that the likelihood function associated with the problem is highly oscillatory, and we propose a computationally efficient technique to maximize this function. Our algorithm first obtains an initial estimate based on a smooth approximate cost function, and then refines this estimate based on the true cost function. Simulation results show that our estimator outperforms a traditional phase-shift based estimator, and that the estimation error approaches the Cramér–Rao bound (CRB) when the signal-to-noise ratio (SNR) increases without bound.**

***Index Terms*—Supercavitation, acoustic sensors, time-delay estimation, maximum likelihood, phase-shift method.**

I. Introduction

THIS paper deals with time-delay estimation using acoustic sensors. The application, that has served as the main motivation for this work is the problem of measuring cavity thickness for underwater supercavitating vehicles (however, the results of this paper can also be applied directly to many other applications such as proximity barrier detection and fluid level measurement [1], [2]). In fact, the maximum speed of the submerged vehicles, by using traditional underwater techniques, is limited up to about 80 m/h. This limitation, however, is being broken by a physical phenomenon called *supercavitation*, which makes it possible for underwater vehicles to travel at hundreds of miles per hour [3], [4]. The core of this technique is to surround the moving object with an envelope of gas so that the contact area between the liquid and the vehicle surface is minimized, and as a consequence the viscous drag is reduced drastically. The feasibility of such vehicles is dependent mainly on the ability to actively control the shape and quality of the gaseous cavity when the vehicle maneuvers at high speeds, and hence an efficient cavity sensing technique is very important. Due to the hard acoustic boundary at the gas/water interface, acoustic-based cavity thickness measurement methods are expected to be superior to other possibilities such as electromagnetic or laser-based methods.

Consider a signal transmitted from an ultrasonic transducer. The emitted signal propagates through the transmission medium (for instance, air or water) and is reflected by the boundary (or a suitable reflector). The reflected signal is received by a receiving transducer (that may be the same as the transmitting transducer). The time-delay of the signal propagating from the transmitter to the receiver is measured and converted into a value proportional to the distance.

Numerous techniques including the pulse-echo and the continuous wave (CW) measurement techniques have been developed for performing the time-delay measurement [5]–[7]. The so-called *pulse-echo method* is based on the estimation of the time-delay between the moment of transmission and the time-of-arrival of the reflected wave. To measure a small distance and to get a high accuracy of the estimate, the sound pulse must be extremely short. However, owing to the high quality factors of the transducers, most existing ultrasound transducers can only generate the pulses with long ringing tails [8]. Therefore, when using a conventional ultrasound transducer, the pulse-echo measurement technique is not useful for close proximity measurements (that is, when the distance between the sensor and the reflector is less than 5 cm).

Another class of distance measurement methods is based on continuous sound wave (CW) generation techniques and overcomes the distance restriction of the conventional pulse-echo method. These methods require that the transducer generate ultrasound continuously and receive the reflected signal simultaneously. The most widely used method within the class of CW measurement techniques is called the impedance or amplitude method, which can be analyzed similar to the Fabry-Perot principle known in optics [9]. In the space between the sensor and the reflector, the emitted and reflected sound waves interfere with each other and a standing wave pattern is generated. The received signal amplitude is maximal or minimal when the waves are in resonance or antiresonance, respectively. The distance between the sensor and the reflector is obtained by measuring the frequency difference between two neighboring resonance peaks or notches. Another CW-based method, referred to as the *phase-shift method*, is much simpler and faster since it only requires two measurements of a phase-shift on two different working frequencies. This method is widely applied in optics [10]–[12]. A traditional estimator for the phase-shift method is described in [6] and is based on the fact that given the two different working frequencies, the difference between the two

Manuscript received February 15, 2001; revised August 15, 2001. This work was supported in part by ONR, Advanced Technology Development for the Control of High-Speed Supercavitating Vehicles, under Grant N00014-00-1-0105 and in part by the Swedish Foundation for Strategic Research (SSF).

X. Li and J. Li are with the Department of Electrical and Computer Engineering, University of Florida, Gainesville, FL 32611 USA (e-mail: li@dsp.ufl.edu).

E. G. Larsson is with the Department of Electrical and Computer Engineering, University of Florida, Gainesville, FL 32611 USA, on leave from the Department of Systems and Control, Uppsala University, Uppsala, Sweden.

M. Sheplak is with the Department of Aerospace Engineering, Mechanics and Engineering Science, University of Florida, Gainesville, FL 32611 USA.

Publisher Item Identifier S 0364-9059(02)00653-2.

Report Documentation Page

Form Approved
OMB No. 0704-0188

1. REPORT DATE	2. REPORT TYPE	3. DATES COVERED
AUG 2001		**00-00-2001 to 00-00-2001**

4. TITLE AND SUBTITLE	5a. CONTRACT NUMBER
Phase-Shift-Based Time-Delay Estimators for Proximity Acoustic Sensors	5b. GRANT NUMBER
	5c. PROGRAM ELEMENT NUMBER
6. AUTHOR(S)	5d. PROJECT NUMBER
	5e. TASK NUMBER
	5f. WORK UNIT NUMBER
7. PERFORMING ORGANIZATION NAME(S) AND ADDRESS(ES) **University of Florida,Department of Electrical and Computer Engineering,Gainesville,FL,32611**	8. PERFORMING ORGANIZATION REPORT NUMBER
9. SPONSORING/MONITORING AGENCY NAME(S) AND ADDRESS(ES)	10. SPONSOR/MONITOR'S ACRONYM(S)
	11. SPONSOR/MONITOR'S REPORT NUMBER(S)

12. DISTRIBUTION/AVAILABILITY STATEMENT
Approved for public release; distribution unlimited

13. SUPPLEMENTARY NOTES

14. ABSTRACT

15. SUBJECT TERMS

16. SECURITY CLASSIFICATION OF:			17. LIMITATION OF ABSTRACT	18. NUMBER OF PAGES	19a. NAME OF RESPONSIBLE PERSON
a. REPORT **unclassified**	b. ABSTRACT **unclassified**	c. THIS PAGE **unclassified**		**10**	

phase-shifts is proportional to the time-delay. However, it turns out that this estimator is not optimal when the signal is known to have a real-valued amplitude. Furthermore, this estimator does not take the noise into account in a proper way.

In this paper, we consider the phase-shift method in the case when the amplitude of the signal is nonnegative unknown, and the measurements are corrupted by colored or nonuniform Gaussian noise. A new time-delay estimator based on a maximum-likelihood approach is derived. However, this estimator requires the solution of an optimization problem whose objective function is highly oscillatory. Inspired by a related work in [13], we propose an approach to obtain an initial time-delay estimate by assuming that the amplitude of the reflected signal is complex-valued and then to refine the initial estimate based on the true cost function. A computationally efficient algorithm, referred to as the direct matching method (DMM), is presented to obtain the refined estimate. As shown in this paper, our algorithm performs much better than the estimator in [6] and the root-mean-squared errors (RMSEs) of the parameter estimates of the new method approach the corresponding Cramér-Rao bounds (CRBs) when the signal-to-noise ratio (SNR) increases without bound. We also show that for the case in which the amplitude is no longer real-valued, but complex-valued with a small phase angle (i.e., in the case of a small model mismatch), the new method can still perform better than the traditional method for a low to moderate SNR.

II. Problem Formulation

Assume that the transmitted ultrasonic signal is a sinusoid:

$$s_t(t) = \sin(2\pi f_1 t + \phi_1) \tag{1}$$

where f_1 is the transmitted frequency and ϕ_1 is the initial phase. When the sound waveform is normally incident on the interface between two media, the wave is partly reflected and partly transmitted into the second medium. The reflection coefficient is defined as $R = p^-/p^+$, where p^+ is the pressure of the incident wave and p^- is the pressure of the reflected wave. This can also be expressed as $R = (z_2 - z_1)/(z_2 + z_1)$, where the z_1 and z_2 are the characteristic impedances of the transmission media [14]. When the impedance of the second medium is much larger than that of the first medium, for instance, when the aerial sound waves impinge onto a water surface, R becomes equal to one, which implies that the reflected signal is an exact replica of the incident signal. Hence, in this case, the signal received by the transducer can be written as

$$s_r(t) = \beta \sin[2\pi f_1(t-\tau) + \phi_1 + \pi] \tag{2}$$

where τ is the round-trip time-delay between the sensor and the reflecting boundary and β is the amplitude, which is considered to be a nonnegative unknown, and π is induced by "half wavelength loss" due to the acoustic hard boundary. Therefore, the phase-shift between the transmitted and received signal due to the time-delay is $2\pi f_1 \tau$. In order to measure this phase-shift, standard IQ processing is performed on the received signal. This means that $s_r(t)$ is demodulated with the in-phase and quadrature components of $s_t(t), \sin(2\pi f_1 t + \phi_1)$ and $\cos(2\pi f_1 t + \phi_1)$, respectively. The demodulated signals are passed through low-pass filters and the real and imaginary parts of $\beta e^{j2\pi f_1 \tau}$ are obtained by measuring the output amplitudes of the two low-pass filters.

Assume that N subsequent and independent measurements are taken using the frequency f_1. Then each measurement value can be modeled as

$$x_1(n) = \beta e^{j2\pi f_1 \tau} + e_1(n), \quad n = 1, 2, \ldots, N \tag{3}$$

where we assume that $e_1(n)$ is a zero-mean circular symmetric complex white (with respect to n) Gaussian random variable with variance σ_1^2. Assume further that a corresponding set of N independent measurements are obtained by transmitting a signal with the known frequency f_2 (without loss of generality, we assume $f_1 < f_2$):

$$x_2(n) = \beta e^{j2\pi f_2 \tau} + e_2(n), \quad n = 1, 2, \ldots, N \tag{4}$$

where $e_2(n)$ is Gaussian noise with variance σ_2^2. We will in general assume that the noise is nonuniform so that $\sigma_1^2 \neq \sigma_2^2$. This modeling accounts for the possibility that the noise level is different at different frequencies, a situation that can, for example, arise from hardware artifacts. Furthermore, we will allow for the possibility that $e_1(n)$ and $e_2(n)$ are correlated, a situation that could arise, for instance, if the two measurements (at time n) on frequency f_1 and f_2 are taken simultaneously using two transducers. We will see that this data model leads not only to a robust estimation algorithm, but is also mathematically efficient.

The data model can be expressed using matrix notation as follows. Define the vector of measurements

$$\mathbf{x}(n) \triangleq [x_1(n) \quad x_2(n)]^T \in \mathcal{C}^{2\times 1} \tag{5}$$

where $(\cdot)^T$ denotes the transpose, let

$$\mathbf{e}(n) \triangleq [e_1(n) \quad e_2(n)]^T \in \mathcal{C}^{2\times 1} \tag{6}$$

be a vector containing the noise samples and let

$$\mathbf{b}(\tau) \triangleq [e^{j2\pi f_1 \tau} \quad e^{j2\pi f_2 \tau}]^T. \tag{7}$$

Then the data model in (3) and (4) can be written in a matrix form as

$$\mathbf{x}(n) = \beta \mathbf{b} + \mathbf{e}(n), \quad n = 1, 2, \ldots, N \tag{8}$$

where $\mathbf{e}(n)_{n=1}^N$ are independently and identically distributed zero-mean circularly symmetric complex Gaussian random vectors with an unknown positive definite covariance matrix

$$\mathbf{Q} = \begin{bmatrix} \sigma_1^2 & \rho\sigma_1\sigma_2 \\ \rho^*\sigma_1\sigma_2 & \sigma_2^2 \end{bmatrix} \tag{9}$$

and here the complex correlation coefficient ρ is defined as

$$\rho = \frac{E(e_1^* e_2)}{\sigma_1 \sigma_2}. \tag{10}$$

Hereafter $E(x)$ is the expected value of x and $(\cdot)^*$ denotes the complex conjugate. The problem of interest in our paper is to estimate $\{\tau, \beta\}$ from $\mathbf{x}(n), n = 1, 2, \ldots, N$.

III. Time Delay Estimation

A. Maximum Likelihood Estimator

The log-likelihood function of $\mathbf{x}(n)$ is proportional to (within an additive constant):

$$\mathcal{L} = -\ln[\det(\mathbf{Q})] - \mathrm{tr}\left\{\mathbf{Q}^{-1}\frac{1}{N}\sum_{n=1}^{N}[\mathbf{x}(n) - \beta\mathbf{b}][\mathbf{x}(n) - \beta\mathbf{b}]^H\right\} \quad (11)$$

where $\det(\cdot)$ denotes the determinant of a matrix, $[\cdot]^H$ denotes the conjugate transpose, and $\mathrm{tr}\{\cdot\}$ stands for the trace of the matrix.

It is easy to show that the matrix $\mathbf{Q}$ that maximizes (11) is (see, e.g., [15], [16])

$$\mathbf{Q} = \frac{1}{N}\sum_{n=1}^{N}[\mathbf{x}(n) - \beta\mathbf{b}][\mathbf{x}(n) - \beta\mathbf{b}]^H. \quad (12)$$

Insertion of (12) into (11) shows that maximizing (11) is equivalent to minimizing

$$\mathcal{L}_1 \triangleq \det\left(\frac{1}{N}\sum_{n=1}^{N}[\mathbf{x}(n) - \beta\mathbf{b}][\mathbf{x}(n) - \beta\mathbf{b}]^H\right) \triangleq \det(\mathbf{G}) \quad (13)$$

where

$$\mathbf{G} \triangleq \frac{1}{N}\sum_{n=1}^{N}[\mathbf{x}(n) - \beta\mathbf{b}][\mathbf{x}(n) - \beta\mathbf{b}]^H. \quad (14)$$

Let

$$\bar{\mathbf{x}} \triangleq \frac{1}{N}\sum_{n=1}^{N}\mathbf{x}(n), \quad (15)$$

and

$$\hat{\mathbf{R}}_{xx} \triangleq \frac{1}{N}\sum_{n=1}^{N}\mathbf{x}(n)\mathbf{x}(n)^H. \quad (16)$$

Then $\mathbf{G}$ can be written as

$$\begin{aligned}\mathbf{G} &= \hat{\mathbf{R}}_{xx} - \beta\mathbf{b}\bar{\mathbf{x}}^H - \beta^*\bar{\mathbf{x}}\mathbf{b}^H + |\beta|^2\mathbf{b}\mathbf{b}^H \\ &= [\beta\mathbf{b} - \bar{\mathbf{x}}][\beta\mathbf{b} - \bar{\mathbf{x}}]^H + \hat{\mathbf{R}}_{xx} - \bar{\mathbf{x}}\bar{\mathbf{x}}^H. \end{aligned} \quad (17)$$

With this notation, the cost function $\mathcal{L}_1$ in (13) can be written as

$$\begin{aligned}\mathcal{L}_1 &= \det[\hat{\mathbf{R}}_{xx} - \bar{\mathbf{x}}\bar{\mathbf{x}}^H + (\beta\mathbf{b} - \bar{\mathbf{x}})(\beta\mathbf{b} - \bar{\mathbf{x}})^H] \\ &= \det(\hat{\mathbf{Q}})\det[\mathbf{I} + \hat{\mathbf{Q}}^{-1}(\beta\mathbf{b} - \bar{\mathbf{x}})(\beta\mathbf{b} - \bar{\mathbf{x}})^H] \\ &= \det(\hat{\mathbf{Q}})[1 + (\beta\mathbf{b} - \bar{\mathbf{x}})^H\hat{\mathbf{Q}}^{-1}(\beta\mathbf{b} - \bar{\mathbf{x}})] \end{aligned} \quad (18)$$

where

$$\hat{\mathbf{Q}} \triangleq \hat{\mathbf{R}}_{xx} - \bar{\mathbf{x}}\,\bar{\mathbf{x}}^H \quad (19)$$

and where we have used the fact that $\det(\mathbf{I} + \mathbf{AB}) = \det(\mathbf{I} + \mathbf{BA})$ whenever the dimensions of $\mathbf{A}$ and $\mathbf{B}$ are conformable [17]. Hence, maximizing $\mathcal{L}$ is equivalent to minimizing

$$\mathcal{L}_2(\tau, \beta) = [\beta\mathbf{b}(\tau) - \bar{\mathbf{x}}]^H\hat{\mathbf{Q}}^{-1}[\beta\mathbf{b}(\tau) - \bar{\mathbf{x}}] \quad (20)$$

which is a highly nonlinear optimization problem.

Before we proceed, let us remark on the following two facts. First, the data model in (8), the related optimization problem of maximizing (11) and its solution are similar to those obtained for the amplitude and phase estimation (APES) filter [18]. Second, it is evident from (20) that the exact ML estimator of (τ, β) reduces to a simple nonlinear least square (NLS) cost function of *pre-whitened* data. Note, however, that $\hat{\mathbf{Q}}$ in (19) is *not* the ML estimate of $\mathbf{Q}$.

We will consider three different cases: β is complex-valued, β is real-valued and β is nonnegative, respectively. Consider first the case where β is an unknown complex-valued scalar. Then minimizing $\mathcal{L}_2(\tau, \beta)$ with respect to τ and β yields the estimates of $\hat{\tau}$ and $\hat{\beta}$, respectively, as

$$\hat{\tau}_{c_1} = \arg\max_{\tau} c_1(\tau) \triangleq \arg\max_{\tau}\frac{|\mathbf{b}^H\hat{\mathbf{Q}}^{-1}\bar{\mathbf{x}}|^2}{\mathbf{b}^H\hat{\mathbf{Q}}^{-1}\mathbf{b}} \quad (21)$$

$$\hat{\beta}_{c_1} = \left.\frac{\mathbf{b}^H\hat{\mathbf{Q}}^{-1}\bar{\mathbf{x}}}{\mathbf{b}^H\hat{\mathbf{Q}}^{-1}\mathbf{b}}\right|_{\tau=\hat{\tau}_{c_1}}. \quad (22)$$

Next, consider the case of a real-valued β. Minimizing $\mathcal{L}_2(\tau, \beta)$ with respect to τ and β yields

$$\hat{\tau}_{c_2} = \arg\max_{\tau} c_2(\tau) \triangleq \arg\max_{\tau}\frac{\mathrm{Re}^2(\mathbf{b}^H\hat{\mathbf{Q}}^{-1}\bar{\mathbf{x}})}{\mathbf{b}^H\hat{\mathbf{Q}}^{-1}\mathbf{b}} \quad (23)$$

$$\hat{\beta}_{c_2} = \left.\frac{\mathrm{Re}(\mathbf{b}^H\hat{\mathbf{Q}}^{-1}\bar{\mathbf{x}})}{\mathbf{b}^H\hat{\mathbf{Q}}^{-1}\mathbf{b}}\right|_{\tau=\hat{\tau}_{c_2}} \quad (24)$$

where $\mathrm{Re}(x)$ is the real part of x. Finally, consider the case when β is a nonnegative unknown. Minimizing $\mathcal{L}_2(\tau, \beta)$ for a fixed τ with respect to β yields

$$\hat{\beta}(\tau) = \frac{\mathrm{Re}(\mathbf{b}^H\hat{\mathbf{Q}}^{-1}\bar{\mathbf{x}})}{\mathbf{b}^H\hat{\mathbf{Q}}^{-1}\mathbf{b}}u\left(\frac{\mathrm{Re}(\mathbf{b}^H\hat{\mathbf{Q}}^{-1}\bar{\mathbf{x}})}{\mathbf{b}^H\hat{\mathbf{Q}}^{-1}\mathbf{b}}\right) \quad (25)$$

where $u(x)$ is the unit step function:

$$u(x) = \begin{cases} 1, & \text{if } x \geq 0 \\ 0, & \text{if } x < 0. \end{cases} \quad (26)$$

Insertion of (25) into (20) gives

$$\begin{aligned}\hat{\tau}_{c_3} &= \arg\max_{\tau} c_3(\tau) \\ &\triangleq \arg\max_{\tau}\frac{\mathrm{Re}^2(\mathbf{b}^H\hat{\mathbf{Q}}^{-1}\bar{\mathbf{x}})}{\mathbf{b}^H\hat{\mathbf{Q}}^{-1}\mathbf{b}}u\left(\frac{\mathrm{Re}(\mathbf{b}^H\hat{\mathbf{Q}}^{-1}\bar{\mathbf{x}})}{\mathbf{b}^H\hat{\mathbf{Q}}^{-1}\mathbf{b}}\right). \end{aligned} \quad (27)$$

Once we have obtained $\hat{\tau}_{c_3}$, the corresponding $\hat{\beta}_{c_3}$ is obtained from (25) as $\hat{\beta}_{c_3} = \hat{\beta}(\hat{\tau}_{c_3})$.

According to the parsimony principle [19], if β is real-valued, the estimates obtained by maximizing $c_2(\tau)$ and $c_3(\tau)$ should be more accurate than those obtained by maximizing $c_1(\tau)$ due to the different constraints on β. Although (23) and (27) are simple one-dimensional search problems, the objective functions $c_2(\tau)$ and $c_3(\tau)$ are highly oscillatory and have numerous closely spaced local maxima which make it very difficult to find the global maximum. In the section below, we present a fast algorithm to cope with these optimization problems.

B. Estimation Algorithm

To solve the optimization problems in previous section, we first introduce the following notation. Let

$$\hat{\mathbf{Q}}^{-1} \triangleq \begin{bmatrix} \gamma_1 & \nu \\ \nu^* & \gamma_2 \end{bmatrix} \tag{28}$$

$$\psi_\nu \triangleq \arg(\nu) \tag{29}$$

$$\bar{x}_i \triangleq \frac{1}{N}\sum_{n=1}^{N} x_i(n), \quad i = 1, 2 \tag{30}$$

$$\psi_{\bar{x}_i} \triangleq \arg(\bar{x}_i), \quad i = 1, 2 \tag{31}$$

where $\hat{\mathbf{Q}}$ is defined in (19) and $\arg(x)$ is the phase of x.

1) Maximization of $c_1(\tau)$: Consider first the optimization problem for the cost function $c_1(\tau)$, which after some straightforward algebra can be written as

$$c_1(\tau) = \frac{A + |B|\cos(\psi + \psi_B)}{\gamma_1 + \gamma_2 + 2|\nu|\cos(\psi + \psi_\nu)} \tag{32}$$

where

$$A \triangleq |\bar{x}_1|^2\left(\gamma_1^2 + |\nu|^2\right) + |\bar{x}_2|^2\left(\gamma_2^2 + |\nu|^2\right) + 2\mathrm{Re}[\bar{x}_1\bar{x}_2^*(\gamma_1 + \gamma_2)\nu^*] \tag{33}$$

$$B \triangleq 2[\nu(|\bar{x}_1|^2\gamma_1 + |\bar{x}_2|^2\gamma_2) + \bar{x}_1\bar{x}_2^*\gamma_1\gamma_2 + \bar{x}_1^*\bar{x}_2\nu^2] \tag{34}$$

$$\psi_B \triangleq \arg(B), \tag{35}$$

$$\psi \triangleq 2\pi(f_2 - f_1)\tau. \tag{36}$$

Differentiating $c_1(\tau)$ with respect to ψ and setting the derivative to zero yields

$$|B|\sin(\psi + \psi_B)[\gamma_1 + \gamma_2 + 2|\nu|\cos(\psi + \psi_\nu)] - [A + |B|\cos(\psi + \psi_B)][2|\nu|\sin(\psi + \psi_\nu)] = 0. \tag{37}$$

Let

$$p \triangleq |B|(\gamma_1 + \gamma_2)\cos(\psi_B) - 2|\nu|A\cos(\psi_\nu) \tag{38}$$

$$q \triangleq |B|(\gamma_1 + \gamma_2)\sin(\psi_B) - 2|\nu|A\sin(\psi_\nu) \tag{39}$$

$$\Psi \triangleq \arg(p + jq). \tag{40}$$

Then the solution of (37) is

$$\hat{\psi} = \arcsin\left(-\frac{2|\nu||B|\sin(\psi_B - \psi_\nu)}{\sqrt{p^2 + q^2}}\right) - \Psi. \tag{41}$$

If it is known *a priori* that $\tau_{\max} < 1/(f_2 - f_1)$, the estimate of τ is

$$\hat{\tau}_{c_1} = \begin{cases} \dfrac{\hat{\psi}}{2\pi(f_2 - f_1)}, & \text{if } \hat{\psi} \geq 0 \\ \dfrac{\hat{\psi} + 2\pi}{2\pi(f_2 - f_1)}, & \text{if } \hat{\psi} < 0. \end{cases} \tag{42}$$

Note that in the special case that it is known that $\mathbf{Q} = \sigma^2\mathbf{I}$ where $\mathbf{I}$ is the identity matrix and $\sigma^2 \triangleq \sigma_1^2 = \sigma_2^2$, the estimator in (42) can be simplified to

$$\hat{\tau}_{c_1} = \begin{cases} \dfrac{\psi_{\bar{x}_2} - \psi_{\bar{x}_1}}{2\pi(f_2 - f_1)}, & \text{if } \psi_{\bar{x}_2} - \psi_{\bar{x}_1} \geq 0 \\ \dfrac{(\psi_{\bar{x}_2} - \psi_{\bar{x}_1}) + 2\pi}{2\pi(f_2 - f_1)}, & \text{if } \psi_{\bar{x}_2} - \psi_{\bar{x}_1} < 0 \end{cases} \tag{43}$$

which is the same expression as for the traditional phase-shift method in [6].

2) DMM: Although a closed-form solution to maximizing $c_1(\tau)$ with respect to τ can be found, it is less accurate than the solution obtained by maximizing $c_2(\tau)$ and $c_3(\tau)$, if β is real-valued. However, it is difficult to maximize $c_2(\tau)$ and $c_3(\tau)$ directly due to the fact that both of them are highly oscillatory with $c_3(\tau)$ being even nonsmooth.

In this paper, we propose to maximize the cost function $c_1(\tau)$ by first obtaining an initial estimate $\hat{\tau}_{c_1}$, and then refine it based on $c_2(\tau)$ or $c_3(\tau)$ respectively. Our algorithm, which doesn't require a search through the parameter space of τ, is described below and will be called the DMM algorithm.

Rewrite the cost function $c_2(\tau)$ as

$$c_2(\tau) = g_1(\tau)\cdot g_2^2(\tau) \tag{44}$$

where

$$g_1(\tau) \triangleq (\mathbf{b}^H\hat{\mathbf{Q}}^{-1}\mathbf{b})^{-1} = [\gamma_1 + \gamma_2 + 2|\nu|\cos(2\pi(f_2 - f_1)\tau + \psi_\nu)]^{-1} \tag{45}$$

and

$$\begin{aligned} g_2(\tau) &\triangleq \mathrm{Re}(\mathbf{b}^H\hat{\mathbf{Q}}^{-1}\bar{\mathbf{x}}) \\ &= \gamma_1|\bar{x}_1|\cos(2\pi f_1\tau - \psi_{\bar{x}_1}) \\ &\quad + \gamma_2|\bar{x}_2|\cos(2\pi f_2\tau - \psi_{\bar{x}_2}) \\ &\quad + |\nu||\bar{x}_1|\cos(2\pi f_2\tau - \psi_{\bar{x}_1} + \psi_\nu) \\ &\quad + |\nu||\bar{x}_2|\cos(2\pi f_1\tau - \psi_{\bar{x}_2} - \psi_\nu). \end{aligned} \tag{46}$$

It can be noted that the denominator of $g_1(\tau)$ contains a sinusoid with (low) frequency $f_2 - f_1$ and that $g_2(\tau)$ is highly oscillatory with an oscillation frequency somewhere between f_1 and f_2. Therefore, the cost function $c_2(\tau)$ is highly oscillatory. Differentiating $c_2(\tau)$ with respect to τ yields

$$c_2'(\tau) = g_1'(\tau)\cdot g_2^2(\tau) + 2g_1(\tau)\cdot g_2(\tau)\cdot g_2'(\tau). \tag{47}$$

Next, we expand $c_2'(\tau)$ around $\hat{\tau}_{c_1}$ to a first-order approximation and find the solution to the equation $c_2'(\tau) = 0$, which corresponds to the local maximum of $c_2(\tau)$ around $\hat{\tau}_{c_1}$. A Taylor series expansion of $g_1(\tau)$ around $\hat{\tau}_{c_1}$ yields to a second-order approximation

$$g_1(\tau) \approx a_0 + a_1(\tau - \hat{\tau}_{c_1}) + a_2(\tau - \hat{\tau}_{c_1})^2 \tag{48}$$

where

$$a_0 \triangleq g_1(\tau)|_{\tau=\hat{\tau}_{c_1}} = [\gamma_1 + \gamma_2 + 2|\nu|\cos(2\pi(f_2 - f_1)\hat{\tau}_{c_1} + \psi_\nu)]^{-1} \tag{49}$$

$$\begin{aligned} a_1 &\triangleq \left.\frac{\partial g_1(\tau)}{\partial\tau}\right|_{\tau=\hat{\tau}_{c_1}} \\ &= 4\pi(f_2 - f_1)|\nu|\sin(2\pi(f_2 - f_1)\hat{\tau}_{c_1} + \psi_\nu)[\gamma_1 \\ &\quad + \gamma_2 + 2|\nu|\cos(2\pi(f_2 - f_1)\hat{\tau}_{c_1} + \psi_\nu)]^{-2} \end{aligned} \tag{50}$$

and

$$\begin{aligned} a_2 &\triangleq \left.\frac{1}{2}\frac{\partial^2 g_1(\tau)}{\partial\tau^2}\right|_{\tau=\hat{\tau}_{c_1}} \\ &= 4\pi^2(f_2 - f_1)^2|\nu|\{\cos(2\pi(f_2 - f_1)\hat{\tau}_{c_1} + \psi_\nu)[\gamma_1 \\ &\quad + \gamma_2 + 2|\nu|\cos(2\pi(f_2 - f_1)\hat{\tau}_{c_1} + \psi_\nu)]^{-2} \\ &\quad + 4|\nu|\sin^2(2\pi(f_2 - f_1)\hat{\tau}_{c_1} + \psi_\nu)[\gamma_1 + \gamma_2 \\ &\quad + 2|\nu|\cos(2\pi(f_2 - f_1)\hat{\tau}_{c_1} + \psi_\nu)]^{-3}\}. \end{aligned} \tag{51}$$

Since β is nonnegative, we have the following approximation for high SNR:

$$2\pi f_i \hat{\tau}_{c_1} \approx 2k_i\pi + \psi_{\bar{x}_i}, \quad i = 1, 2 \tag{52}$$

where

$$k_i = \left\lfloor \frac{2\pi f_i \hat{\tau}_{c_1} - \psi_{\bar{x}_i}}{2\pi} \right\rfloor, \quad i = 1, 2 \tag{53}$$

with $\lfloor \cdot \rfloor$ denoting rounding to the nearest integer. Note that the information that $\beta \geq 0$ is used explicitly here. In a small range around $\hat{\tau}_{c_1}$, (52) yields the following approximation:

$$\cos[2\pi f_i(\tau - \hat{\tau}_{c_1})] \approx \cos(2\pi f_i \tau - \psi_{\bar{x}_i} - 2k_i\pi) \approx 1, \quad i = 1, 2 \tag{54}$$

and

$$\begin{aligned} \sin[2\pi f_i(\tau - \hat{\tau}_{c_1})] &\approx \sin(2\pi f_i \tau - \psi_{\bar{x}_i} - 2k_i\pi) \\ &\approx 2\pi f_i \tau - \psi_{\bar{x}_i} - 2k_i\pi, \quad i = 1, 2. \end{aligned} \tag{55}$$

Then $g_2(\tau)$ and $g_2'(\tau)$ can be expanded in their first-order approximations around $\hat{\tau}_{c_1}$ as

$$g_2(\tau) \approx b_0 + b_1\tau \tag{56}$$

and

$$g_2'(\tau) \approx d_0 + d_1\tau \tag{57}$$

where

$$\begin{aligned} b_0 = {} & |\bar{x}_1|[\gamma_1 + |\nu|\cos(\bar{\psi}) - |\nu|\sin(\bar{\psi})(\psi_{\bar{x}_2} + 2k_2\pi)] \\ & + |\bar{x}_2|[\gamma_2 + |\nu|\cos(\bar{\psi}) + |\nu|\sin(\bar{\psi})(\psi_{\bar{x}_1} + 2k_1\pi)] \end{aligned} \tag{58}$$

$$b_1 = 2\pi|\nu|\sin(\bar{\psi})(f_2|\bar{x}_1| - f_1|\bar{x}_2|) \tag{59}$$

$$\begin{aligned} d_0 = {} & 2\pi|\nu|\sin(\bar{\psi})(f_2|\bar{x}_1| - f_1|\bar{x}_2|) \\ & + 2\pi f_1(\psi_{\bar{x}_1} + 2k_1\pi)[|\nu||\bar{x}_2|\cos(\bar{\psi}) + \gamma_1|\bar{x}_1|] \\ & + 2\pi f_2(\psi_{\bar{x}_2} + 2k_2\pi)[|\nu||\bar{x}_1|\cos(\bar{\psi}) + \gamma_2|\bar{x}_2|] \end{aligned} \tag{60}$$

$$\begin{aligned} d_1 = {} & -4\pi^2|\bar{x}_1|\left[|\nu|f_2^2\cos(\bar{\psi}) + \gamma_1 f_1^2\right] \\ & - 4\pi^2|\bar{x}_2|\left[|\nu|f_1^2\cos(\bar{\psi}) + \gamma_2 f_2^2\right] \end{aligned} \tag{61}$$

where

$$\bar{\psi} = \psi_{\bar{x}_1} - \psi_{\bar{x}_2} - \psi_\nu. \tag{62}$$

Therefore, around $\hat{\tau}_{c_1}$, $c_2'(\tau)$ can be approximately expressed as

$$\begin{aligned} c_2'(\tau) \approx {} & [a_1 + 2a_2(\tau - \hat{\tau}_{c_1})](b_0 + b_1\tau)^2 \\ & + 2[a_0 + a_1(\tau - \hat{\tau}_{c_1})](b_0 + b_1\tau)(d_0 + d_1\tau). \end{aligned} \tag{63}$$

Simplifying (63), neglecting the second-order term of $\tau - \hat{\tau}_{c_1}$, and setting it to zero, we obtain the refined solution, as shown in (64) at the bottom of the page, where

$$b_{01} = b_0 + b_1\hat{\tau}_{c_1} \tag{65}$$

and

$$d_{01} = d_0 + d_1\hat{\tau}_{c_1}. \tag{66}$$

As a final remark, we note that if it is known a priori that $\mathbf{Q} = \sigma^2\mathbf{I}$, i.e., $\gamma_1 = \gamma_2$ and $\nu = 0$, and if the SNR is high, i.e., $|\bar{x}_1| \approx |\bar{x}_2|$, (64) can be simplified to

$$\begin{aligned} \hat{\tau}_{\mathrm{DMM}}|_{\mathbf{Q}=\sigma^2\mathbf{I}} = {} & \frac{f_1^2}{f_1^2 + f_2^2}\left(\frac{2k_1\pi + \psi_{\bar{x}_1}}{2\pi f_1}\right) \\ & + \frac{f_2^2}{f_1^2 + f_2^2}\left(\frac{2k_2\pi + \psi_{\bar{x}_2}}{2\pi f_2}\right). \end{aligned} \tag{67}$$

Equation (67) can be interpreted as a weighted summation of the two estimates of τ obtained via f_1 and f_2 separately.

The steps of the DMM algorithm are summarized as follows:

1) Estimate $\hat{\mathbf{Q}}$ via (19). Invert $\hat{\mathbf{Q}}$ to obtain γ_1, γ_2 and ν [see (28)].
2) Obtain an initial estimate of $\hat{\tau}_{c_1}$ via (42).
3) Estimate k_1 and k_2 via (53).
4) Compute $a_0, a_1, a_2, b_0, b_1, d_0, d_1$ via (49)–(51) and (58)–(62).
5) Obtain the final estimate $\hat{\tau}_{\mathrm{DMM}}$ via (64).

Once the final estimate $\hat{\tau}$ is obtained, computing the estimate $\hat{\beta}$ is straightforward via (24).

3) Analysis of Model Errors: In practical measurement scenarios, due to the complex measurement environment and in particular the nonideal rigid wall reflection and inhomogeneities of the transmission media, it may not be entirely correct to model β as a nonnegative number. In fact, it can be argued that β should be modeled as a complex-valued number $\beta = |\beta|e^{j\psi_\beta}$ where ψ_β is a small phase angle. In this case, the estimate $\hat{\tau}_{\mathrm{DMM}}$, which is obtained by assuming β is nonnegative, will be biased due to the model mismatch. It can be shown that for the special case $\mathbf{Q} = \sigma^2\mathbf{I}$ in (67), the bias and the mean-squared errors (MSE) of the estimate $\hat{\tau}_{\mathrm{DMM}}$ are

$$\mathrm{Bias}(\hat{\tau}_{\mathrm{DMM}}) = E(\hat{\tau}_{\mathrm{DMM}} - \tau|\tau) = \frac{f_1 + f_2}{2\pi(f_1^2 + f_2^2)}\psi_\beta \tag{68}$$

and

$$\begin{aligned} \mathrm{MSE}(\hat{\tau}_{\mathrm{DMM}}) = E[(\hat{\tau}_{\mathrm{DMM}} - \tau)^2|\tau] = {} & \frac{\sigma^2}{8N|\beta|^2\pi^2(f_1^2 + f_2^2)} \\ & + \left[\frac{f_1 + f_2}{2\pi(f_1^2 + f_2^2)}\psi_\beta\right]^2. \end{aligned} \tag{69}$$

It is clear from the above equations that both $\mathrm{Bias}(\hat{\tau}_{\mathrm{DMM}})$ and $\mathrm{MSE}(\hat{\tau}_{\mathrm{DMM}})$ increase as ψ_β increases.

IV. Numerical Examples

In this section, we present several computer simulations to illustrate the performance of our proposed algorithm. The performance of our algorithm is compared to the Cramér-Rao bound

$$\hat{\tau}_{\mathrm{DMM}} = \hat{\tau}_{c_1} - \frac{a_1 b_{01}^2 + 2a_0 b_{01} d_{01}}{2\left(a_2 b_{01}^2 + a_1 b_1 b_{01} + a_0 b_1 d_{01} + a_0 b_{01} d_1 + a_1 b_{01} d_{01}\right)} \tag{64}$$

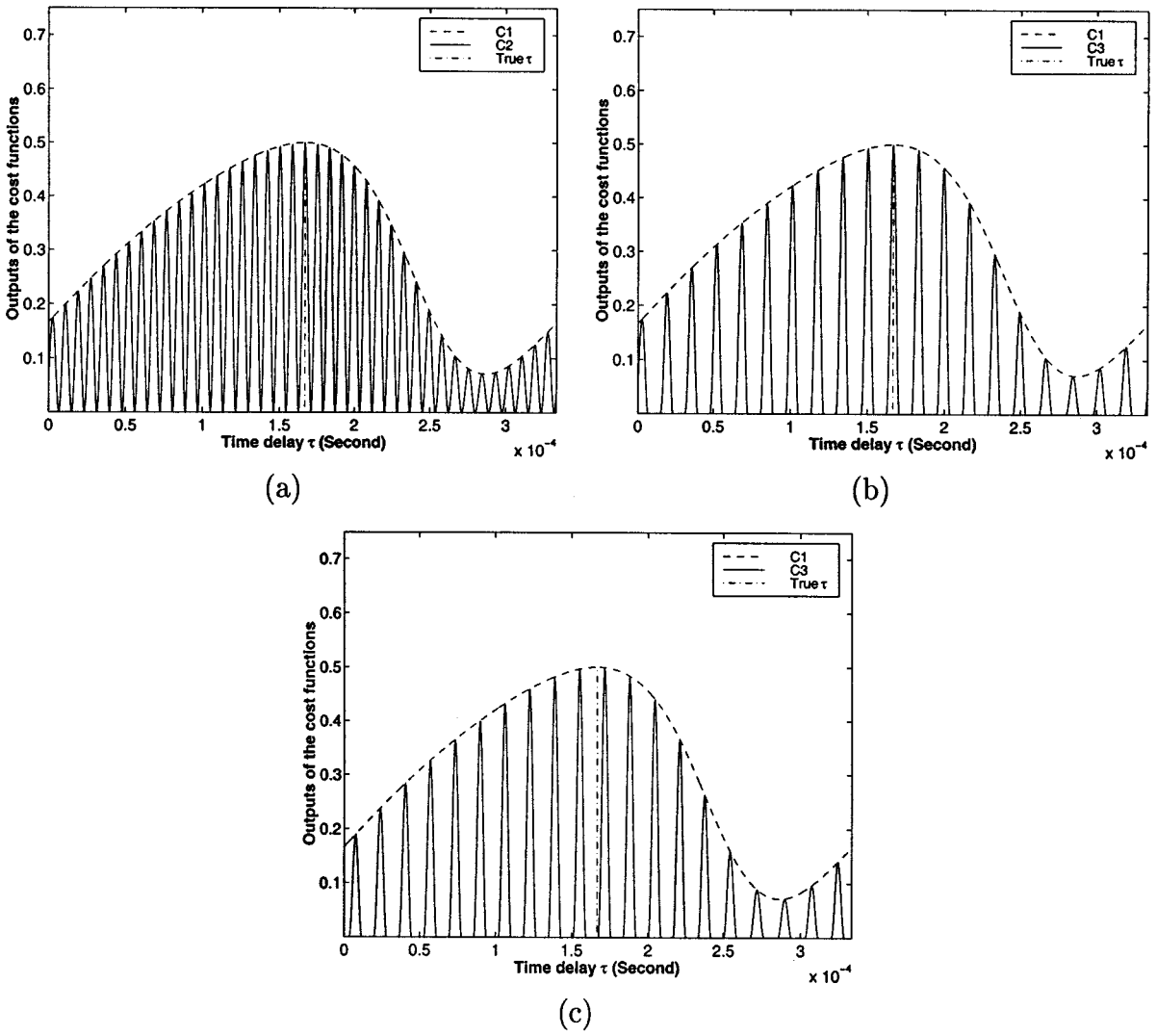

Fig. 1. Comparison of the cost functions $c_1(\tau), c_2(\tau)$ and $c_3(\tau)$ for different assumptions on the signal amplitude β. No noise is present. True time-delay is 1.67×10^{-4} s. (a), (b) β is nonnegative, three cost functions share same global maximum. (c) β is complex-valued, the global maximum of $c_3(\tau)$ deviates away from the true location of τ.

(CRB), which gives the minimum attainable variance for any unbiased estimator. The CRB for our problem is derived in Appendix A. In the simulations below, we use $N = 10, \beta = 0.5, f_1 = 60$ kHz, $f_2 = 63$ kHz, $\tau = 1.67 \times 10^{-4}$ s (corresponding to 0.028 m if the sound speed is 340 m/s). The RMSE of each estimate is obtained by 500 Monte Carlo trials and the SNR is defined as $2\beta^2/(\sigma_1^2 + \sigma_2^2)$.

Fig. 1 illustrates the cost functions $c_1(\tau), c_2(\tau)$ and $c_3(\tau)$. As shown in Fig. 1(a) and (b), $c_1(\tau), c_2(\tau)$ and $c_3(\tau)$ share the same global maximum if β is nonnegative. Note that both $c_2(\tau)$ and $c_3(\tau)$ are highly oscillatory, and also that $c_3(\tau)$ has many nondifferentiable points. On the other hand, $c_1(\tau)$ is the envelope of $c_2(\tau)$ and $c_3(\tau)$ and is in fact quite smooth. It is expected that maximizing $c_2(\tau)$ or $c_3(\tau)$ can yield a much more accurate estimate than maximizing $c_1(\tau)$, due to the sharper peaks of $c_2(\tau)$ or $c_3(\tau)$. Moreover, since $c_2(\tau)$ has more closely spaced local maxima than $c_3(\tau)$, it is intuitively expected that $c_2(\tau)$ is more sensitive to noise in a certain SNR range than $c_3(\tau)$ is. If β is complex-valued, as shown in Fig. 1(c), the global maxima of $c_2(\tau)$ and $c_3(\tau)$ deviate from the true location of τ (for simplicity, only $c_3(\tau)$ is shown in this figure). Hence, the estimates based on $c_2(\tau)$ or $c_3(\tau)$ will be biased due to the model mismatch.

Fig. 2(a) illustrates the RMSEs of the different methods for the estimates of τ. The noise covariance matrix used here is $\mathbf{Q} = \sigma^2\mathbf{I}$ and five different methods are compared. The first is called "C1" and uses the closed-form solution in (42) to maximize cost function $c_1(\tau)$. The second and the third methods are based on maximizing $c_2(\tau)$ and $c_3(\tau)$ by a 1-D search method, and are referred to as "C2" and "C3," respectively. The 1-D search is performed in two steps, with an initial estimate via (42), followed by a fine search using the $f\min$ function in MATLAB. The fourth is "C3 (White)," which is a special case of C3, where the $\hat{\mathbf{Q}}$ is set to an identity matrix, that is, we assume the noise is white. The last method is the DMM given by (64) [(67) is not used in any of our simulations]. It can be noted that C1 cannot approach the real CRB even when the SNR goes to infinity. However, both C2, C3, and DMM approach the real CRB when the SNR increases. Note that the threshold effect for C3 and DMM occurs earlier than for C2, which is intuitively expected

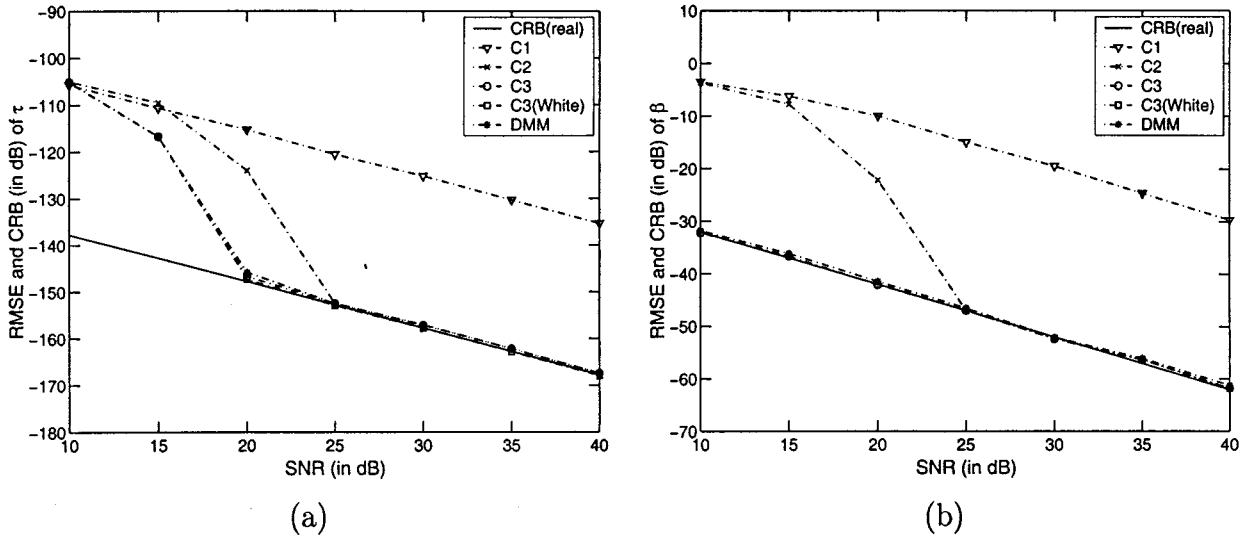

Fig. 2. Comparison of the RMSEs and CRBs for estimating (a) τ; (b) β when the signal amplitude is assumed to be complex-valued (C1), real-valued (C2), and nonnegative (C3). The noise covariance matrix is $\mathbf{Q} = \sigma^2\mathbf{I}$.

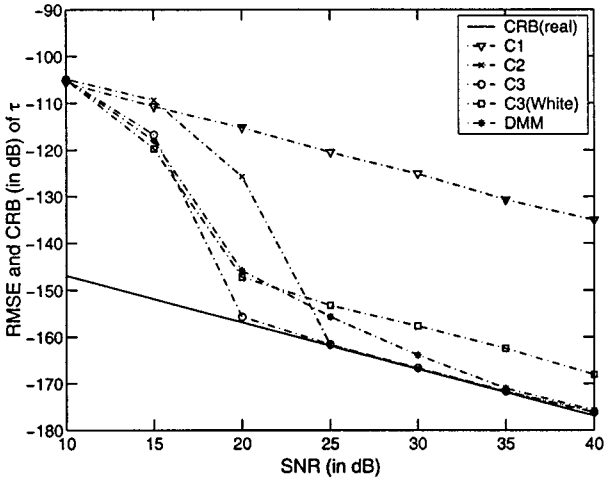

Fig. 3. Comparison of the RMSEs and CRBs for estimating τ when the signal amplitude is assumed to be complex-valued (C1), real-valued (C2), and nonnegative (C3). The noises of the two channels are correlated with each other and have different variances.

since both C3 and DMM use the information that β is nonnegative. Note also that the performances of C3, C3(White) and DMM are almost the same, despite the fact that C3 and DMM do not take advantage of the prior knowledge of the noise. In other words, the robustness against the colored or nonuniform noise offered by our data model and algorithm comes at a negligible cost (or rather a negligible performance loss in the case $\mathbf{Q} = \sigma^2\mathbf{I}$). The reason for this is related to the fact that our estimation problem is *decoupled* in the sense that the Fisher information matrix is block diagonal (cf. Appendix A). Fig. 2(b) shows the corresponding estimates of β.

Fig. 3 illustrates the RMSEs of the different methods for the estimates of τ when the noise covariance matrix is $\mathbf{Q} = \begin{bmatrix} \sigma_1^2 & -0.93\sigma_1\sigma_2 j \\ -0.93\sigma_1\sigma_2 j & \sigma_2^2 \end{bmatrix}$ where $\sigma_2^2/\sigma_1^2 = 2$. Note that the performance of DMM is close to that of C3 and approaches the real CRB as the SNR increases. If the information of $\mathbf{Q}$ is not used, as shown by C3 (white), there is a gap of 8 dB from the real CRB, no matter how high the SNR is.

As a further illustration of the robustness of our algorithm, Fig. 4(a) shows the performance of the C3 and DMM as a function of the absolute value of the correlation coefficient ρ by fixing the $\mathrm{SNR} = 35$ dB, $\arg(\rho) = \pi/2$ and $\sigma_1^2 = \sigma_2^2$. The figure shows that both C3 and DMM are close to the real CRB, however, C3 (White) deviates from the real CRB when $|\rho|$ approaches unity (i.e., when the noises in the two channels become highly correlated). Fig. 4(b) shows the performance of the τ estimators as a function of the ratio of the two variances σ_2^2/σ_1^2 by fixing $\mathrm{SNR} = 35$ dB and $\rho = 0$. It can be noted that C3 and DMM can still achieve the real CRB, whereas C3 (white) deviates from the real CRB when the ratio increases. The interpretation of this is that our estimator has ability to estimate the noise level on the two different frequencies, and to combine the measurements optimally taking the different noise levels into account.

From Figs. 3 and 4, we can see that our new estimator has the ability to adapt to an unknown noise model. Both C2, C3, and DMM can achieve the real CRB as long as the SNR is above a certain threshold. However, DMM is computationally more efficient than C2 and C3 since it does not require any search.

Finally, in Fig. 5 we illustrate the performance of DMM when β is complex-valued with a small phase angle. The noise covariance matrix is $\mathbf{Q} = \sigma^2\mathbf{I}$. Due to the model mismatch, our estimates are biased, and can therefore not approach the real CRBs as the SNR increases. However, if the phase angle ψ_β is small and the SNR is low to moderate, which means that the estimation error caused by the noise is larger than the constant bias due to the model mismatch, DMM still performs better than the traditional method. When the SNR increases, the constant bias caused by the model mismatch becomes dominant compared to the error caused by the noise, and the traditional method outperforms DMM. Note that the RMSE of $\hat{\beta}$ for the traditional method is lower than the corresponding CRBs at the low SNRs, which is due to the fact that it is a biased estimator.

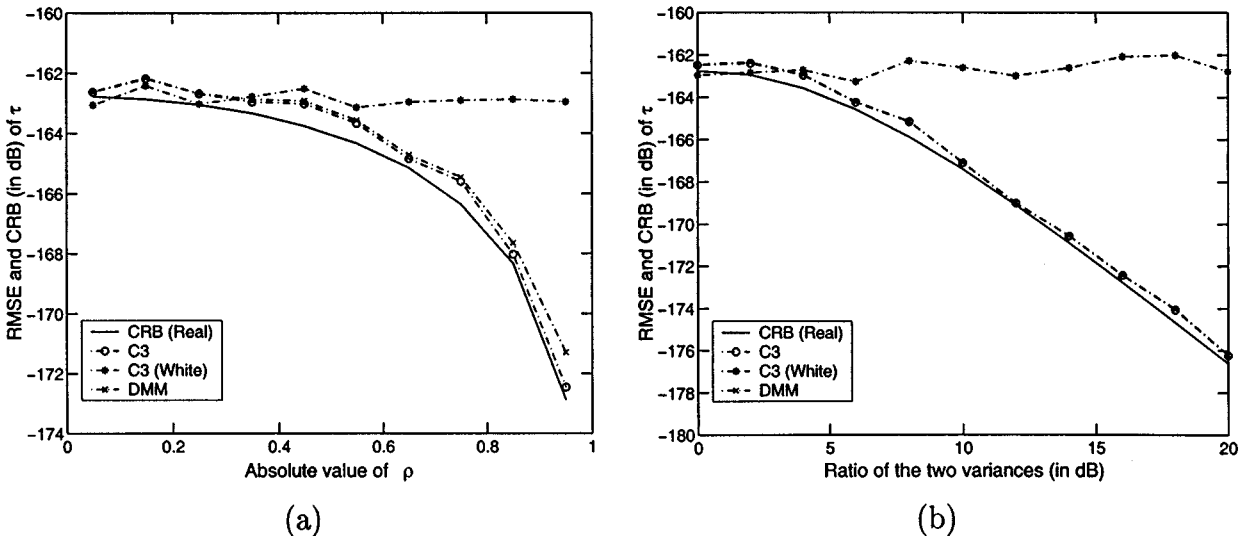

Fig. 4. Comparison of the RMSEs and CRBs for estimating τ. (a) As a function of the absolute value of ρ with $\arg(\rho) = \pi/2$. (b) As a function of σ_2^2/σ_1^2 with $\rho = 0$. The signal amplitude is assumed to be nonnegative and $\mathrm{SNR} = 35$ dB.

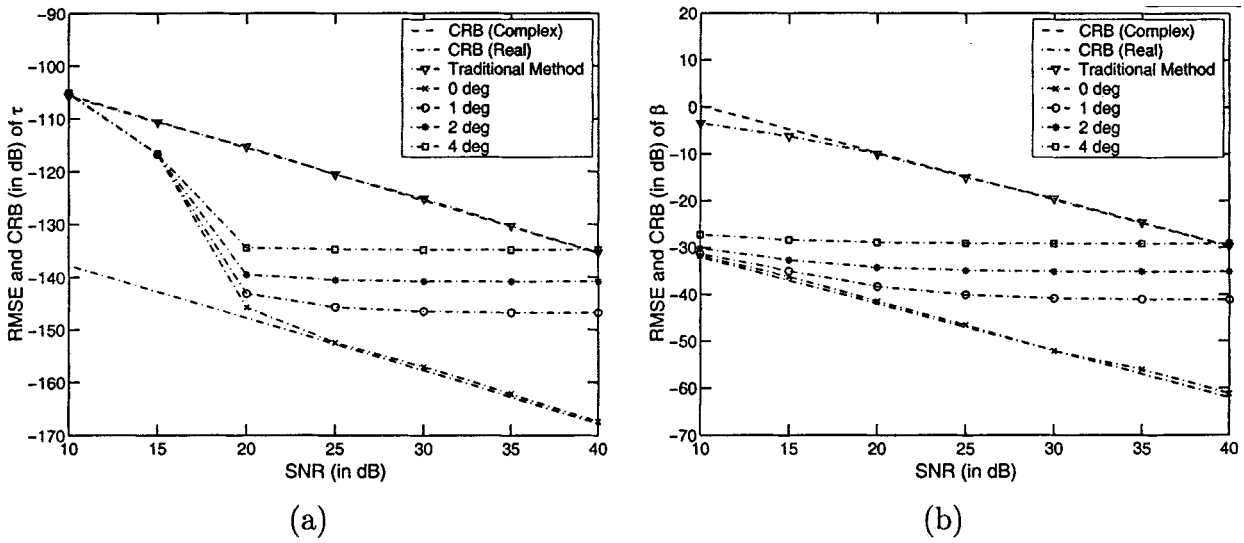

Fig. 5. Comparison of the RMSEs and CRBs by using DMM to estimate (a) τ and (b) β. Here the phase angle of β is 0°, 1°, 2°, 4°, respectively. The noise covariance matrix is $\mathbf{Q} = \sigma^2\mathbf{I}$.

V. Conclusion

In this paper, we have presented a new time-delay estimator for the phase-shift method. We have considered the case when the amplitude of the signal is nonnegative unknown and the measurements are corrupted by Gaussian noise with unknown covariance. To deal with the induced optimization problem, whose cost function is highly oscillatory, we propose a method called DMM that first finds an initial estimate of the unknown parameter by maximizing a smoother cost function, and then refines this estimate based on the true cost function. The RMSEs of the estimates obtained by using our new algorithm approach the corresponding CRBs as the SNR increases. Since DMM does not require any search over the parameter space, it is suitable for a practical implementation. We also show that in the case of a model mismatch, if the phase angle of the reflection coefficient is small, the DMM can still perform better than the traditional method for low to moderate SNR. Although the motivation for our work has been cavity thickness measurements for supercavitation systems, the results of this paper are applicable to many other proximity distance measurement applications as well.

Appendix A
Derivation of CRBs

We outline below the derivation of CRBs for the parameter estimates of the following data model:

$$\mathbf{x}(n) = \beta\mathbf{b} + \mathbf{e}(n), \quad n = 1, 2, \ldots, N \tag{70}$$

where $\mathbf{b} = [e^{j2\pi f_1\tau}\ e^{j2\pi f_2\tau}]^T$.

In (70) the additive noise vectors $\mathbf{e}(n), n = 1, 2, \ldots, N$ are assumed to be independent zero-mean Gaussian random vectors with an unknown covariance matrix $\mathbf{Q}$. The data samples $\mathbf{x}(n), n = 1, 2, \ldots, N$ are independent and the unknown parameters in the estimation problem are the real and imaginary parts of β (for complex-valued β) or simply the amplitude of β (for real-valued β), the time-delay τ and the unknown elements of $\mathbf{Q}$. Let η be a vector containing those parameters. The CRB

inequality states that provided the estimates are unbiased, the covariance matrix of the estimated parameter vectors η is lower bounded by the inverse of the Fisher information matrix FIM^{-1}. The FIM can be computed by the extended Slepian-Bang's formula [17]:

$$\{\mathrm{FIM}\}_{ij} = N\,\mathrm{tr}(\mathbf{Q}^{-1}\mathbf{Q}_i'\mathbf{Q}^{-1}\mathbf{Q}_j') + 2N\,\mathrm{Re}[(\beta\mathbf{b})_i'^H\mathbf{Q}^{-1}(\beta\mathbf{b})_j'] \quad (71)$$

(here $\mathbf{X}_i'$ denotes the derivative of $\mathbf{X}$ with respect to the ith unknown parameter). Note that the FIM is a block diagonal matrix since $\mathbf{Q}$ does not depend on the parameters in $\beta\mathbf{b}(\tau)$, and $\beta\mathbf{b}(\tau)$ does not depend on the elements in $\mathbf{Q}$. Hence, the CRB of the estimates of the delay and the amplitude can be determined from the second term of the right side of (71).

We first derive the CRB s for the case of a complex-valued β. Let

$$\eta_{\mathrm{sc}} = [\mathrm{Re}(\beta) \quad \mathrm{Im}(\beta) \quad \tau]^T \quad (72)$$

where $\mathrm{Im}(x)$ denotes the imaginary part of x, be a vector of the signal parameters (i.e., the parameters in the upper left block of the FIM). Define

$$\mu_1' \triangleq \frac{\partial\mu}{\partial\mathrm{Re}(\beta)} = \mathbf{b} \quad (73)$$

$$\mu_2' \triangleq \frac{\partial\mu}{\partial\mathrm{Im}(\beta)} = j\mathbf{b} \quad (74)$$

$$\mu_3' \triangleq \frac{\partial\mu}{\partial\tau} = j2\pi\beta\begin{bmatrix} f_1 e^{j2\pi f_1\tau} \\ f_2 e^{j2\pi f_2\tau}\end{bmatrix} \quad (75)$$

and let

$$\mathbf{F} = [\mu_1' \quad \mu_2' \quad \mu_3']. \quad (76)$$

Then

$$\mathrm{CRB}(\eta_{\mathrm{sc}}) = [2N\,\mathrm{Re}(\mathbf{F}^H\mathbf{Q}^{-1}\mathbf{F})]^{-1} \quad (77)$$

which is easily evaluated numerically. If $\sigma^2 \triangleq \sigma_1^2 = \sigma_2^2$ and $\rho = 0$, simplifying (77) yields

$$\mathrm{CRB}_\beta = \mathrm{CRB}_{\mathrm{Re}(\beta)} + \mathrm{CRB}_{\mathrm{Im}(\beta)} = \frac{\sigma^2}{4N}\left(1 + 2\frac{f_1^2+f_2^2}{(f_1-f_2)^2}\right) \quad (78)$$

and

$$\mathrm{CRB}_\tau = \frac{\sigma^2}{4N|\beta|^2\pi^2(f_1-f_2)^2}. \quad (79)$$

Clearly, for maximal accuracy, $f_2 - f_1$ should be as large as possible. Note however that $f_2 - f_1 < (1/\tau_{\max})$ [cf. the remark before (42)].

Second, we derive the CRBs for real-valued β. Let

$$\eta_{\mathrm{sr}} = [\beta \quad \tau]. \quad (80)$$

Define

$$\mu_1' \triangleq \frac{\partial\mu}{\partial\beta} = \mathbf{b} \quad (81)$$

$$\mu_2' \triangleq \frac{\partial\mu}{\partial\tau} = j2\pi\beta\begin{bmatrix} f_1 e^{j2\pi f_1\tau} \\ f_2 e^{j2\pi f_2\tau}\end{bmatrix}. \quad (82)$$

Let

$$\mathbf{F} = [\mu_1' \quad \mu_2']. \quad (83)$$

Then

$$\mathrm{CRB}(\eta_{\mathrm{sr}}) = [2N\mathrm{Re}(\mathbf{F}^H\mathbf{Q}^{-1}\mathbf{F})]^{-1}. \quad (84)$$

If $\sigma^2 \triangleq \sigma_1^2 = \sigma_2^2$ and $\rho = 0$, simplifying (84) yields

$$\mathrm{CRB}_\beta = \frac{\sigma^2}{4N} \quad (85)$$

and

$$\mathrm{CRB}_\tau = \frac{\sigma^2}{8N\beta^2\pi^2(f_1^2+f_2^2)}. \quad (86)$$

In general, the frequency difference is determined by the maximum distance we want to measure. Therefore, once $|f_1 - f_2|$ is fixed, we can choose large f_1 and f_2 to decrease the real CRB of τ. Note however that the lower real CRB we design, the higher SNR is required to approach it.

Note that in the case when $\mathbf{Q} = \sigma^2\mathbf{I}$, according to (79) and (86), the ratio of the CRBs of τ for complex-valued β and for real-valued β is

$$\frac{\mathrm{CRB}_{\mathrm{complex}}}{\mathrm{CRB}_{\mathrm{real}}} = \frac{2(f_1^2+f_2^2)}{(f_1-f_2)^2}. \quad (87)$$

This ratio is directly related to the ratio of the oscillation frequencies of $c_1(\tau)$ and $c_2(\tau)$, respectively, and therefore to the sharpness of the peaks of $c_1(\tau)$ and $c_2(\tau)$. This confirms the heuristic reasoning in Section IV which concludes that the cost function with the sharpest peak should give the most accurate estimate.

REFERENCES

[1] *Handbook of Measurement Science*, Wiley, New York, 1982.

[2] R. C. Turner, P. A. Fuierer, R. E. Newnham, and T. R. Shrout, "Materials for high temperature acoustic and vibration sensors: A review," *Applied Acoust.*, vol. 41, pp. 299–324, 1994.

[3] S. Ashley, "Wrap drive underwater," *Sci. Amer.*, vol. 284, no. 5, pp. 70–79, 2001.

[4] J. D. Hrubes, "High-speed imaging of supercavitating underwater projectiles," *Experiments in Fluids*, vol. 30, pp. 57–64, 2001.

[5] F. E. Gueuning, M. Varlan, C. E. Eugene, and P. Dupuis, "Accurate distance measurement by an autonomous ultrasonic system combining time-of-flight and phase-shift methods," *IEEE Trans. Instrument. Measure.*, vol. 46, pp. 1236–1240, Dec. 1997.

[6] M. R. Hornung and O. Brand, *Micromachined Ultrasound-Based Proximity Sensors*. Boston, MA: Kluwer, 1999.

[7] A. Grennberg and M. Sandell, "Estimation of subsample time delay differences in narrowband ultrasonic echoes using the hilbert transform correlation," *IEEE Trans. Ultrason., Ferroelect., Freq. Contr.*, vol. 41, pp. 588–595, Sept. 1994.

[8] H. Baltes, W. Göpel, and J. Hesse, *Sensors Update*. New York: Wiley, 1998.

[9] E. Hecht and A. Zajac, *Optics*. Reading, MA: Addison-Wesley, 1974.

[10] T. Bosch and M. Lescure, "Selected papers on laser distance measurement," *SPIE Milestone Series*, vol. MS 115, 1995.

[11] B. Journet and S. Poujouly, "High resolution laser range-finder based on phase-shift measurement method," in *Proc. SPIE*, vol. 3520, 1998, pp. 123–132.

[12] J. Rzepka, J. Pienkowski, H. Pawolka, and S. Sambor, "Two-frequency laser interferometer with phase shift measurement," *Optica Applicata*, vol. XXVII, no. 4, pp. 251–254, 1997.

[13] R. Wu and J. Li, "Time-delay estimation via optimizing highly oscillatory cost functions," *IEEE J. Ocean. Eng.*, vol. 23, pp. 235–244, July 1998.

[14] D. T. Blackstock, *Fundamentals of Physical Acoustics*, New York: Wiley, 2000.

[15] J. Li, B. Halder, P. Stoica, and M. Viberg, "Computationally efficient angle estimation for signals with known waveforms," *IEEE Trans. Signal Processing*, vol. 43, pp. 2154–2163, Sept. 1995.
[16] M. Cedervall and R. L. Moses, "Efficient maximum likelihood DOA estimation for signals with known waveforms in the presence of multipath," *IEEE Trans. Signal Processing*, vol. 45, pp. 808–811, Mar. 1997.
[17] P. Stoica and R. L. Moses, *Introduction to Spectral Analysis*. Upper Saddle River, NJ: Prentice-Hall, 1997. 07 458.
[18] J. Li and P. Stoica, "An adaptive filtering approach to spectral estimation and SAR imaging," *IEEE Trans. Signal Processing*, vol. 44, pp. 1469–1484, June 1996.
[19] T. Söderström and P. Stoica, *System Identification*, London, U.K: Prentice-Hall, 1989.

Xi Li (S'01) received the B.Sc and Ph.D. degrees in electrical engineering from Nanjing University of Science and Technology (NUST), Nanjing, China, in 1995 and 1999, respectively.Since May 2000, he has been a Research Assistant with the Department of Electrical and Computer Engineering, University of Florida, Gainesville, working toward the Ph.D. degree majoring in electrical engineering and minoring in aerospace and mechanics engineering.

His research interests include spectral estimation, and signal processing for acoustic and radar applications.

Erik G. Larsson received the M.Sc. degree in applied physics and electrical engineering from Linköping University, Linköping, Sweden, in 1997. In 1999 he joined the Department Systems and Control, Uppsala University, Uppsala, Sweden, where he is currently pursuing the Ph.D. degree.

During 1998–1999, he was a research engineer with Ericsson Radio Systems AB, Stockholm, Sweden, where he was involved in the algorithm design and standardization of location services for the GSM system. He is currently on leave from Uppsala University and is visiting the Department of Electrical and Computer Engineering, University of Florida, Gainesville. His research interests include statistical signal processing, wireless communications, spectral analysis and radar applications.

Mark Sheplak received the B.S. degree in 1989, the M.S. degree in 1992, and the Ph.D. degree in 1995 in mechanical engineering from Syracuse University, Syracuse, NY. During his Ph.D. studies, he was a G.S.R.P. Fellow at NASA-LaRC in Hampton, VA from 1992 to 1995.

He is currently an Assistant Professor with the Department of Aerospace Engineering, Mechanics and Engineering Science, University of Florida (UF). Gainesville. Prior to joining UF in 1998, he was a Postdoctoral Associate with the Massachusetts Institute of Technology's Microsystems Technology Laboratories, Cambridge, MA from 1995–1998. His current research focuses on the design, fabrication, and characterization of high-performance, instrumentation-grade, MEMS-based sensors and actuators that enable the measurement, modeling, and control of various physical properties.

Jian Li (S'87–M'91–SM'97) received the M.Sc. and Ph.D. degrees in electrical engineering from The Ohio State University, Columbus, in 1987 and 1991, respectively.

From April 1991 to June 1991, she was an Adjunct Assistant Professor with the Department of Electrical Engineering, The Ohio State University. From July 1991 to June 1993, she was an Assistant Professor with the Department of Electrical Engineering, University of Kentucky, Lexington. Since August 1993, she has been with the Department of Electrical and Computer Engineering, University of Florida, Gainesville, where she is currently a Professor. Her current research interests include spectral estimation, array signal processing, and signal processing for wireless communications and radar.

Dr. Li is a member of Sigma Xi and Phi Kappa Phi. She received the 1994 National Science Foundation Young Investigator Award and the 1996 Office of Naval Research Young Investigator Award. She is currently an Associate Editor for IEEE TRANSACTIONS ON SIGNAL PROCESSING and a Guest Editor for *Multidimensional Systems and Signal Processing*.